Persistent and transient spectral hole burning in Pr^{3+}- and Eu^{3+}-doped silicate glasses

Th. Schmidt*
Center for the Study of Excited States of Molecules, Huygens and Gorlaeus Laboratories, University of Leiden, 2300 RA Leiden, The Netherlands

R.M. Macfarlane
IBM Almaden Research Center, 650 Harry Road, San Jose, California 95120

S. Völker†
Center for the Study of Excited States of Molecules, Huygens and Gorlaeus Laboratories, University of Leiden, 2300 RA Leiden, The Netherlands

(Received 21 July 1994)

Persistent and time-resolved transient holes were burnt into the $^1D_2 \leftarrow {}^3H_4$ transition of Pr^{3+} and the $^5D_0 \leftarrow {}^7F_0$ transition of Eu^{3+} in silicate glasses. The holewidths were studied as a function of burning-fluence density, wavelength, and temperature between 0.4 and 12 K. Transient holes arising from optical pumping of ground-state nuclear hyperfine levels were found for both ions at $T < 3$ K. Their lifetime decreases with increasing temperature. They are accompanied by symmetrically placed antiholes. For Eu^{3+}, two pairs of antiholes were found which are attributed to the two europium isotopes, ^{151}Eu and ^{153}Eu. For Pr^{3+}, an additional mechanism leading to persistent hole burning dominates above 3 K. The holewidth follows a $T^{(1.3\pm0.1)}$ dependence for Pr^{3+} and a $T^{(1.0\pm0.1)}$ dependence for Eu^{3+}. The temperature dependence is the same as that of the contribution of the two-level systems to the specific heat measured on the same samples and in the same temperature range. The quadrupole splittings of the $^7F_0$ ground state and the crystal-field splittings of the $^7F_1$ and $^7F_2$ levels of Eu^{3+} as a function of excitation wavelength indicate that the strength of the noncubic component of the crystal field varies monotonically for excitation across the $^5D_0 \leftarrow {}^7F_0$ absorption band, falling to zero at the long wavelength edge. The hole width shows a similar variation with excitation frequency. No influence of the experimental time scale on the hole width was detected for either sample between 10^{-2} and 10^2 s.

I. INTRODUCTION

Considerable work has been carried out in the last several years to understand the dynamics of glasses. One approach has been to study the interaction of an electronically excited impurity (molecule or ion) with its surrounding amorphous host. It has been found that the temperature dependence and magnitude of line broadening is very different from that in crystals below ~ 40 K. The first optical experiments on inorganic glasses doped with rare-earth ions at low temperature were performed on Eu^{3+} in a silicate glass by fluorescence line-narrowing (FLN) spectroscopy between 8 and 90 K.[1] The results revealed a linewidth which was more than 1 order of magnitude larger than in crystals at about 80 K, and its temperature dependence was found to be quadratic, instead of T^7 or exponential as in crystals. Such a T^2 dependence was also found for other rare-earth ions in inorganic glasses between 10 and 800 K by FLN (Refs. 2–7) and for Nd^{3+} in a silicate glass between 1.6 and 70 K by picosecond accumulated photon echoes.[8]

The homogeneous linewidth of the $^1D_2 \leftarrow {}^3H_4$ transition of Pr^{3+} in silicate glass, however, was reported to follow a linear T dependence between 1.6 and 20 K when studied by hole-burning and accumulated photon echoes,[9] whereas the $^4F_{3/2} \leftarrow {}^4I_{9/2}$ transition of Nd^{3+} in fused silica yielded a $T^{1.3}$ dependence between 0.1 and 1 K as measured by two-pulse nanosecond photon echoes.[10] On the other hand, hole-burning studies of organic glassy systems[11] and porous silica glass[12] doped with organic molecules have shown that a $T^{1.3}$ dependence of the holewidth, extrapolated to zero burning-fluence density, is generally found below 20 K and down to 0.3 K. By contrast, Eu^{3+} in organic amorphous hosts yielded an exponential dependence between 0.3 and 4.2 K.[13]

Current theories of optical dephasing[14,15] predict that the temperature dependence of the homogeneous linewidth is determined by the energy dependence of the density of states of the two-level systems (TLS) of the glass. This is because the coupling between the optical transition and the TLS is modulated by absorption and emission of phonons, and this leads to a dependence of the form T^α with $\alpha = 1-2$.[11,15] Although the models do not predict the exact T dependence for a given amorphous system, it is expected that this dependence should be the same for the homogeneous linewidth and the contribution of the TLS to the specific heat, C_v^{TLS}.

Due to the limited amount of available data on homo-

geneous linewidths for doped inorganic glasses at very low temperatures, we decided to investigate two systems, Pr^{3+} and Eu^{3+} in silicate glasses, by means of spectral hole-burning. We have studied the widths, shapes, and positions of holes burnt into the $^1D_2 \leftarrow ^3H_4$ transition of Pr^{3+} and the $^5D_0 \leftarrow ^7F_0$ transition of Eu^{3+} as a function of burning-fluence density and excitation wavelength, for temperatures between 0.4 and 12 K, and compared the T dependence of the "effective" homogeneous linewidth, Γ_{hom} (equal to one-half of the holewidth at low fluence), with that of C_v^{TLS}. Two types of hole-burning mechanisms, a persistent and a transient one, are active for Pr^{3+} in silicate glass, whereas Eu^{3+} only shows transient hole burning which is due to optical pumping of the nuclear quadrupole levels.[9] The temperature dependence of the holewidth is independent of the hole-burning mechanism. We were also able to distinguish the two isotopes of europium, ^{151}Eu and ^{153}Eu, from the position of antiholes and have studied this position as a function of excitation wavelength.

An increase of Γ_{hom} with decreasing excitation wavelength within the inhomogeneously broadened $^5D_0 \leftarrow ^7F_0$ transition of Eu^{3+} has been reported in the literature for various inorganic glasses at room temperature.[16] This observation was interpreted in terms of a variation of the coupling strength between the ion and the TLS with the lattice.[16] Also the fluorescence lifetime of the $^5D_0$ state was reported to vary with the crystal-field strength for different sites within the inhomogeneously broadened absorption band.[17] In this work we have observed an increase of the holewidth with decreasing wavelength for Eu^{3+} at liquid-helium temperature, which we attribute to the same crystal-field effect as in Refs. 16 and 17. By contrast, we have not observed any variation of the holewidth within the $^1D_2 \leftarrow ^3H_4$ transition of Pr^{3+}. Finally, we have studied the holewidths for Eu^{3+} and Pr^{3+} for different experimental time scales between 20 ms and 100 s in search of spectral diffusion in silicate glasses and found no evidence for it on this time span.

II. EXPERIMENT

The Eu^{3+}- and Pr^{3+}-doped silicate glasses had the following compositions: 74.75% SiO_2, 15% Na_2O, 5% BaO, 5% ZnO, and 0.25% Eu_2O_3, and 59.9% SiO_2, 27.5% Li_2O, 10% CaO, 2.5% Al_2O_3, and 0.1% Pr_2O_3. Fluorescence and excitation spectra were obtained by exciting the samples with a pulsed nitrogen-laser-pumped dye laser (Molectron UV-22, DL 200, rhodamine 6G dye, bandwidth $\sim 0.7 cm^{-1}$), or a cw Ar^+-laser-pumped dye laser (Coherent CR 599, rhodamine 6G dye, bandwidth $\sim 1\ cm^{-1}$) and detecting the fluorescence by means of a 0.85 m double monochromator (Spex 1402, resolution $\sim 2\ cm^{-1}$). Time-resolved fluorescence was recorded, after wavelength selection with the double monochromator, using a transient digitizer (LeCroy 9540, 300 MHz bandwidth).

A cw single-frequency dye-laser (Coherent CR 599-21, rhodamine 6G dye, frequency jitter $\Gamma_{laser} \sim 2$ MHz, amplitude stabilized to $\leq 0.5\%$) was used to burn and subsequently probe the holes. Typical burning-fluence densities used in these experiments at various temperatures are listed in Table I. The holes were probed by means of fluorescence-excitation spectroscopy: after burning, the laser was attenuated by a factor of 20 to 100 and its frequency scanned over the absorption band while the fluorescence signal was detected using a cooled photomultiplier (EMI 9658R) in combination with appropriate cutoff filters (Schott RG 645-6 mm for Pr^{3+}, and Schott RG 610-6 mm for Eu^{3+}). In some experiments where transient holes were probed, two single-frequency dye lasers were used, one for burning at a fixed frequency and the other for probing the hole. The frequency of the second laser was scanned across the hole profile.

Long-lived holes (lifetime $\tau_{hole} \geq 50$ s) were recorded in a single scan in 50 s after burning for 1–1000 s, using a current amplifier (Keithley 610 CR), an analog-to-digital converter and a personal computer. Short-lived holes ($\tau_{hole} \leq 20$ s) were recorded in a time between 10 and 100 ms after the burn pulse (t_{burn}=5 ms–10 s) by means of time-resolved hole burning (for details, see Ref. 18). In order to obtain short burn and probe pulses, the laser was gated by an acousto-optic modulator (AOM). In the present setup, which was slightly modified with respect to that of Ref. 18, a single AOM (Coherent 305A, carrier frequency 40 MHz) was used instead of two. In this way experimental difficulties which previously arose using two laser beams, like overlapping them at the sample, were overcome. In order to use the same beam for burning and probing, the electronics of the rf driver of the AOM was modified in such a manner that the output amplitude of the diffracted laser beam was controlled by a second input signal. To avoid detection of persistent holes, the laser frequency was shifted after each burn-probe cycle to a new frequency range covering up to 30 GHz. The procedure was repeated at different frequencies until the desired averaging (10–1000 times, depending on the signal-to-noise ratio) was completed.

The "effective" homogeneous linewidth, Γ_{hom}, which may be larger than the real homogeneous linewidth due to spectral diffusion (see Sec. III F), was determined from the holewidth, Γ_{hole}. The latter was measured as a function of burning-fluence density, $P_b t_b/A$, where P_b is the burning power, t_b the burning time, and A the area of the laser spot on the sample. The holes were fitted with a Lorentzian curve. The extrapolation value of $\frac{1}{2}\Gamma_{hole}$ for $P_b t_b/A \rightarrow 0$, after subtracting the laser jitter of ~ 2 MHz, was taken as the value of Γ_{hom}, or "effective" homogeneous linewidth.

Figure 1(a) shows typical holes burnt into the $^5D_0 \leftarrow ^7F_0$ transition of Eu^{3+} at 580 nm and the $^1D_2 \leftarrow ^3H_4$ transition of Pr^{3+} at 606 nm, at 1.2 K, for

TABLE I. Burning-fluence densities (J/cm^2) used to obtain holes about 1-2% deep for Pr^{3+} and Eu^{3+} in silicate glasses at various temperatures.

	T =0.4 K	T =1.2 K	T =4.2 K	T =11 K
Pr^{3+}	3×10^{-3}	2×10^{-2}	9×10^{2}	2×10^{5}
Eu^{3+}	6×10^{-3}	2×10^{-3}	4×10^{-1}	–

different burning-fluence densities, $P_b t_b/A$. For Pr^{3+}, a holewidth of $\Gamma_{hole} = (86 \pm 5)$ MHz with a depth D=1.7% was obtained at the lowest value of $P_b t_b/A = 2 \times 10^{-2}$ J/cm^2, while the hole broadens to $\Gamma_{hole} = (267 \pm 22)$ MHz and deepens to D =3.1% at $P_b t_b/A = 2 \times 10^2$ J/cm^2. A significantly smaller holewidth was obtained for Eu^{3+}, $\Gamma_{hole} = (28 \pm 3)$ MHz and depth D=1.5% at the lowest burning-fluence density of 2×10^{-3} J/cm^2.

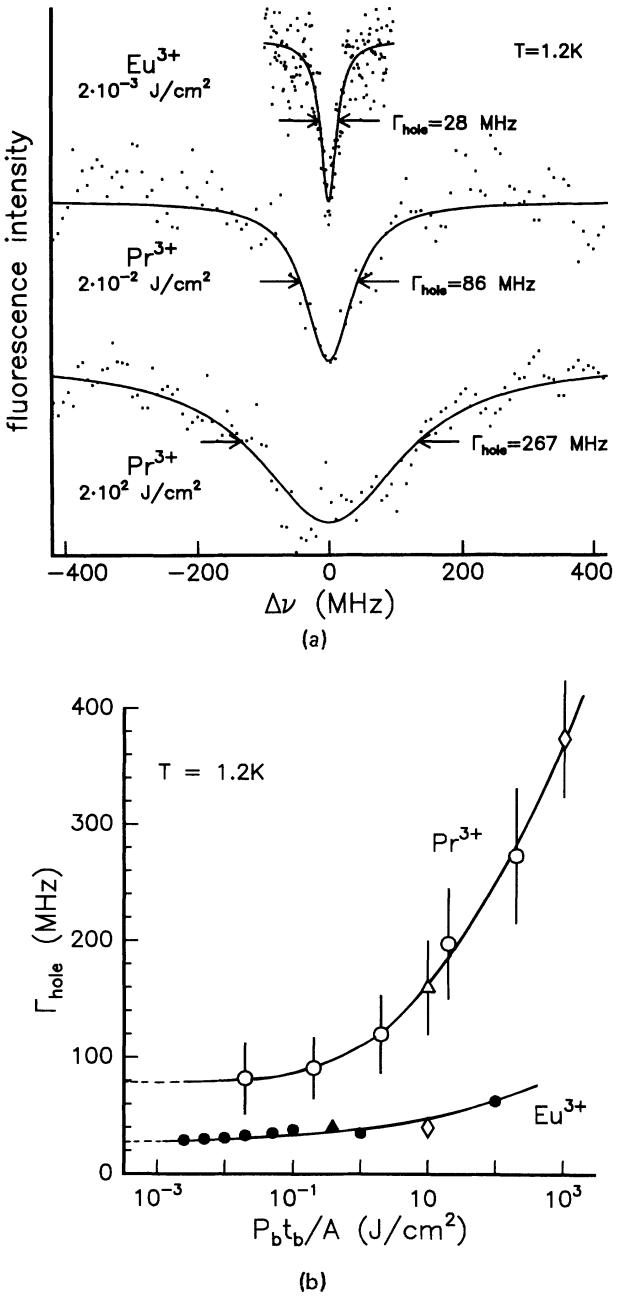

FIG. 1. (a) Holes burnt into the $^5D_0 \leftarrow {}^7F_0$ transition of Eu^{3+} and the $^1D_2 \leftarrow {}^3H_4$ transition of Pr^{3+} in silicate glasses at 1.2 K for different burning-fluence densities, at 580 and 606 nm, respectively. The solid curves represent Lorentzian fits to the data points. (b) Holewidth, Γ_{hole}, as a function of burning-fluence density, $P_b t_b/A$, for Pr^{3+}- and Eu^{3+}-doped silicate glasses at 1.2 K. [Optical transitions as in (a).]

The holewidth, Γ_{hole}, has been plotted as a function of the logarithm of the burning-fluence density, $P_b t_b/A$, in Fig. 1(b). The value of the latter was varied from about 2×10^{-2} J/cm^2 to 2×10^2 J/cm^2 for Pr^{3+}, and from 2×10^{-3} J/cm^2 to 10^2 J/cm^2 for Eu^{3+}. The result of an increase in burning-fluence density of 4 orders of magnitude is a broadening of Γ_{hole} by a factor of about 4 for Pr^{3+}, and a factor of 2 for Eu^{3+}. The points marked with diamonds and triangles were taken from Refs. 9 and 19, respectively. These results prove that there is no contradiction between the values of Γ_{hole} previously reported and those presented here, since the apparent discrepancies are only due to the different burning-fluence densities used. The value for Eu^{3+} at 1.6 K reported in Ref. 9, Γ_{hole}=50 MHz for $P_b t_b/A = 5-100$ J/cm^2, is also consistent with the data of Fig. 1(b) if a linear temperature dependence were assumed (see Sec. III E), and thus Γ_{hole}=37 MHz at 1.2 K.

From the extrapolation of Γ_{hole} for $P_b t_b/A \rightarrow 0$, and after subtracting the laser jitter of 2 MHz, we obtained $\Gamma_{hom} = (38 \pm 5)$ MHz for Pr^{3+} and $\Gamma_{hom} = (13 \pm 2)$ MHz for Eu^{3+}, at 1.2 K. This procedure was used to determine the value of Γ_{hom} at each temperature and wavelength.

The experiments at $T > 4.2$ K were performed in a He-flow cryostat (Leybold-Heraeus). Between 1.2 and 4.2 K, a ^{4}He-bath cryostat was used in which the temperature was controlled by means of the vapor-pressure of the ^{4}He. For temperatures below 1.2 K, a ^{3}He insert was placed into the bath cryostat.[20] The temperature was measured using calibrated carbon resistors in contact with the sample, which allowed a determination of the temperature with an accuracy of 0.01 to 0.05 K, depending on the temperature range.

III. RESULTS AND DISCUSSION

A. Optical spectra

The absorption spectrum of the $^1D_2 \leftarrow {}^3H_4$ transition of Pr^{3+} in silicate glass at 1.2 K is given in Fig. 2(a) (dashed line) between 560 and 610 nm.[21] The band, which is inhomogeneously broadened, consists of the overlap of the five crystal-field components of the first electronically $^1D_2$ excited state[9] [see energy-level diagram on the left of Fig. 2(a)]. The fluorescence spectrum [Fig. 2(a), full line], excited at 580 nm, originates from the lowest crystal-field component of the $^1D_2$ state because fast nonradiative relaxation occurs between the higher crystal-field levels. This is confirmed by the observation that the fluorescence spectrum does not depend on excitation wavelength when pumping into higher crystal-field components between 570 and 600 nm (not shown). The broad emission bands between 600 and 640 nm are due to the overlap of the nine crystal-field components of the $^3H_4$ ground state [Fig. 2(a), left]. Holes were burnt into the lowest $^1D_2$ component between 598 and 606 nm [shaded area in Fig. 2(a)]. The nuclear hyperfine splittings [Fig. 2(a), left] are of the order of a few tens to hundreds of MHz (Refs. 22 and 23) and cannot be distinguished in these spectra.

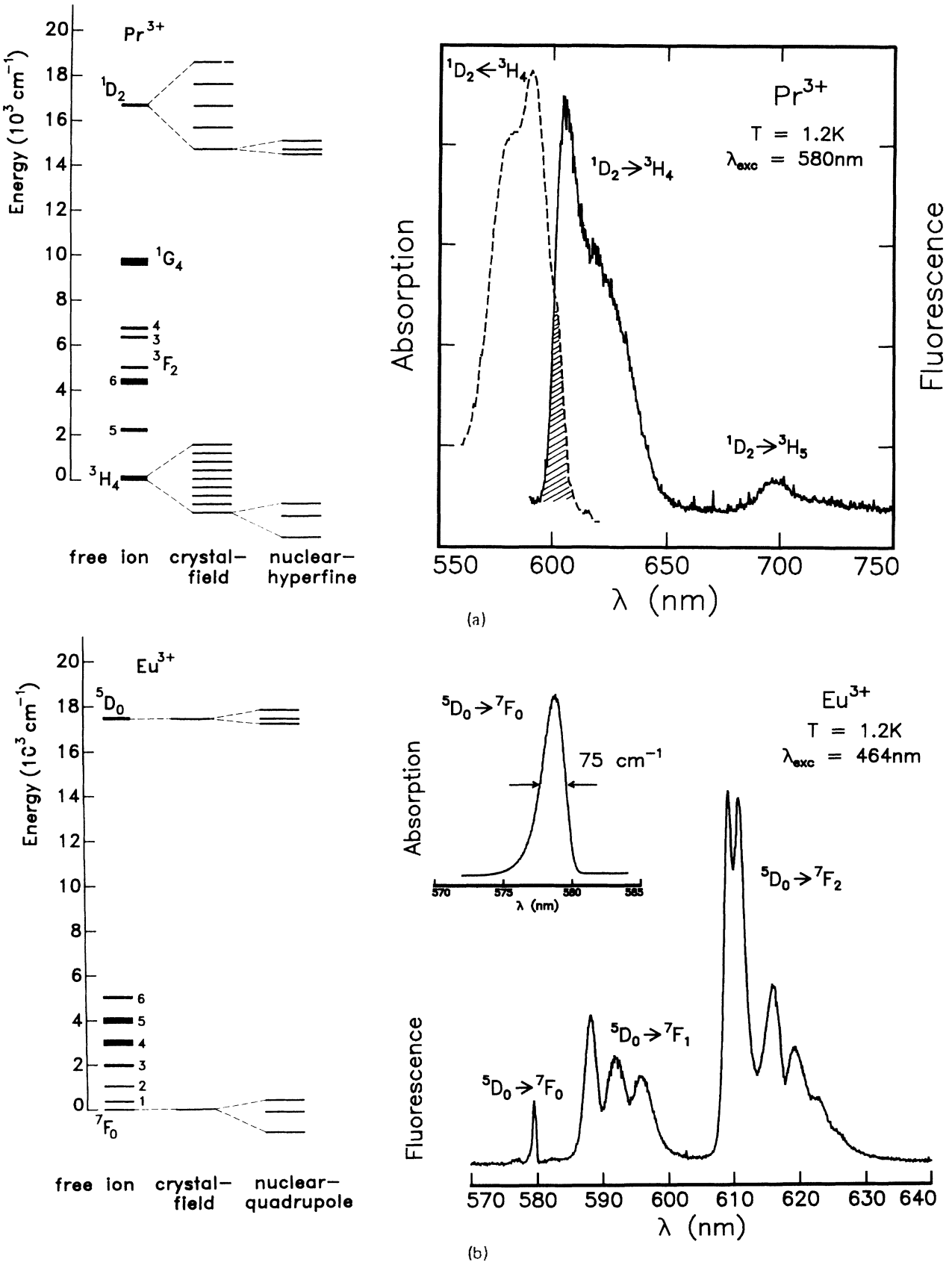

FIG. 2. (a) Left energy levels (shown schematically); and right, absorption (dashed) and fluorescence (solid) spectra of Pr^{3+} in silicate glass at 1.2 K. The fluorescence spectrum was excited in the $^1D_2 \leftarrow {}^3H_4$ transition at 580 nm. (b) as (a) for Eu^{3+} in silicate glass at 1.2 K. The fluorescence spectrum was excited in the $^5D_2 \leftarrow {}^7F_0$ transition at 464 nm.

The excitation and fluorescence spectra of the $^5D_0 \leftrightarrow {}^7F_0$ transition of Eu^{3+} in silicate glass at 1.2 K consist of a single band arising from the nondegenerate nature of the electronic levels involved [see Fig. 2(b), left].[21] This band, which has a width of $\sim$75 cm^{-1}, is inhomogeneously broadened due to variations in the local environment of the different Eu^{3+} ions.[17] The fluorescence spectrum, excited into the $^5D_2 \leftarrow {}^7F_0$ transition at 464 nm, shows several bands which originate from transitions between the $^5D_0$ level and various ^7F_n levels [Fig. 2(b), left]. The nuclear quadrupole splittings are of the order of tens to hundreds of MHz (Refs. 23–26) and are obviously not visible.

In Fig. 3 a three-dimensional plot is shown with a series of fluorescence spectra, between 570 and 640 nm, of Eu^{3+} in silicate glass at 1.5 K. Each spectrum was excited with the laser at a different wavelength within the $^5D_0 \leftarrow {}^7F_0$ band, from 570 to 582 nm. The fluorescence spectra excited at $\lambda_{exc} \leq 576$ nm (Fig. 3, front spectra) are enlarged by a factor of 30 with respect to those excited at $\lambda_{exc} > 576$ nm (Fig. 3, back spectra). The shape and position of the individual components of the $^5D_0 \rightarrow {}^7F_1$ fluorescence transition (585–600 nm) and of the $^5D_0 \rightarrow {}^7F_2$ transition (600–630 nm) vary strongly with excitation wavelength within the $^5D_0 \leftarrow {}^7F_0$ absorption band, as previously found for other glasses.[17,27]

The difference in energy, ΔE, between the position of an individual fluorescence component and the excitation energy is plotted in Fig. 4(a) as a function of excitation energy for the $^5D_0 \rightarrow {}^7F_1$ transition, and in Fig. 4(b) for the $^5D_0 \rightarrow {}^7F_2$ transition of Eu^{3+} in silicate glass at 1.5 K. On the long-wavelength side of the $^5D_0 \leftarrow {}^7F_0$ absorption band, at $\lambda_{exc} \sim 582$ nm, the individual crystal-field components tend to converge to a common point at $\Delta E \sim 320$ cm^{-1} for the $^5D_0 \rightarrow {}^7F_1$ transition (see also Fig. 3, back spectra), and to two points at $\Delta E \sim 800$ and ~ 1050 cm^{-1} for the $^5D_0 \rightarrow {}^7F_2$ transition. The variation of ΔE with excitation energy amounts to $|\, d\Delta E/d\tilde{\nu}_{exc} \,| \sim 1$ cm^{-1}/cm^{-1}, which is of the same order as found for other Eu^{3+}-doped glasses.[17,27] Such spectral shifts have been attributed in Refs. 17 and 27 to the variation of the local crystal-field strength of the Eu^{3+} ions in the glass. From the fact that the $^5D_0 \rightarrow {}^7F_1$ bands tend to converge to a triply degenerate state [Fig. 4(a)] and the $^5D_0 \rightarrow {}^7F_2$ bands to a doubly and a triply degenerate state [Fig. 4(b)] at low excitation energy, we infer that the ions on the red wing of the $^5D_0 \leftarrow {}^7F_0$ absorption band at $\sim$582 nm have a local symmetry which is approximately cubic. Thus, the low-symmetry component of the crystal field increases toward the blue side of the band. A similar conclusion was reached in the literature,[17,27] where a crystal-field analysis had been performed for Eu^{3+} in two different glasses using a point-charge model and assuming a lowering of the local symmetry from O_h to C_{2v}. Since the optical transition is electric-dipole forbidden in cubic symmetry, this may account for the asymmetric shape of the absorption band which drops sharply on the low-energy side.

B. Hole-burning mechanism

So far only short-lived holes had been reported for Eu^{3+} in a silicate glass at 1.6 K and persistent holes for Pr^{3+} in another silicate glass.[9] In the present study we have found a second type of hole-burning mechanism for the latter system and confirmed the already known mechanism for the former.

Pr^{3+} in silicate glass shows persistent or long-lived ($\tau_{hole} > 1$ h) holes (PHB) between 1.2 and 12 K and transient ($\tau_{hole} < 10$ min) holes (THB) between 0.4 and 2.5 K. Since the burning-fluence densities needed for Pr^{3+} at $T > 1.2$ K are much larger than those needed at $T \leq 1.2$ K (see Table I), we conclude that the burning efficiency for THB is much higher than that for PHB. The temperature dependence of Γ_{hom}, however, does not depend on the hole-burning mechanism involved, as will be shown below (Sec. III E). We have verified this for temperatures between 1.2 and 2.5 K where both mechanisms are simultaneously active.

Eu^{3+} in silicate glass, on the contrary, only undergoes THB which we have observed between 0.4 and 4.2 K. We were not able to detect persistent holes in this sample, not even with 1000 times higher burning-fluence densities than those used to burn short-lived holes.

Whereas the PHB mechanism for Pr^{3+} in silicate glass has been attributed to a photo-induced rearrangement of the local structure of the glass surrounding the ions,[9] the

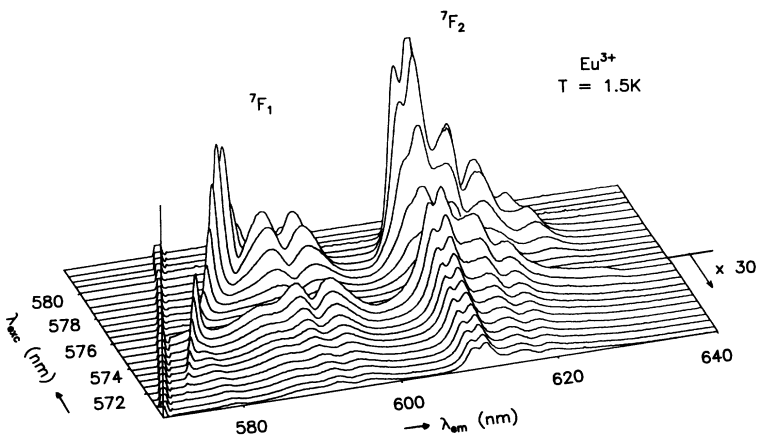

FIG. 3. Fluorescence spectra of the $^5D_0 \rightarrow {}^7F_1$ and $^5D_0 \rightarrow {}^7F_2$ transitions of Eu^{3+} in silicate glass at 1.5 K excited at different wavelengths within the $^5D_0 \leftarrow {}^7F_0$ absorption band. The spectra excited at $\lambda_{exc} \leq 576$ nm (in the front) are enlarged by a factor of 30 with respect to those excited at $\lambda_{exc} > 576$ nm (in the back).

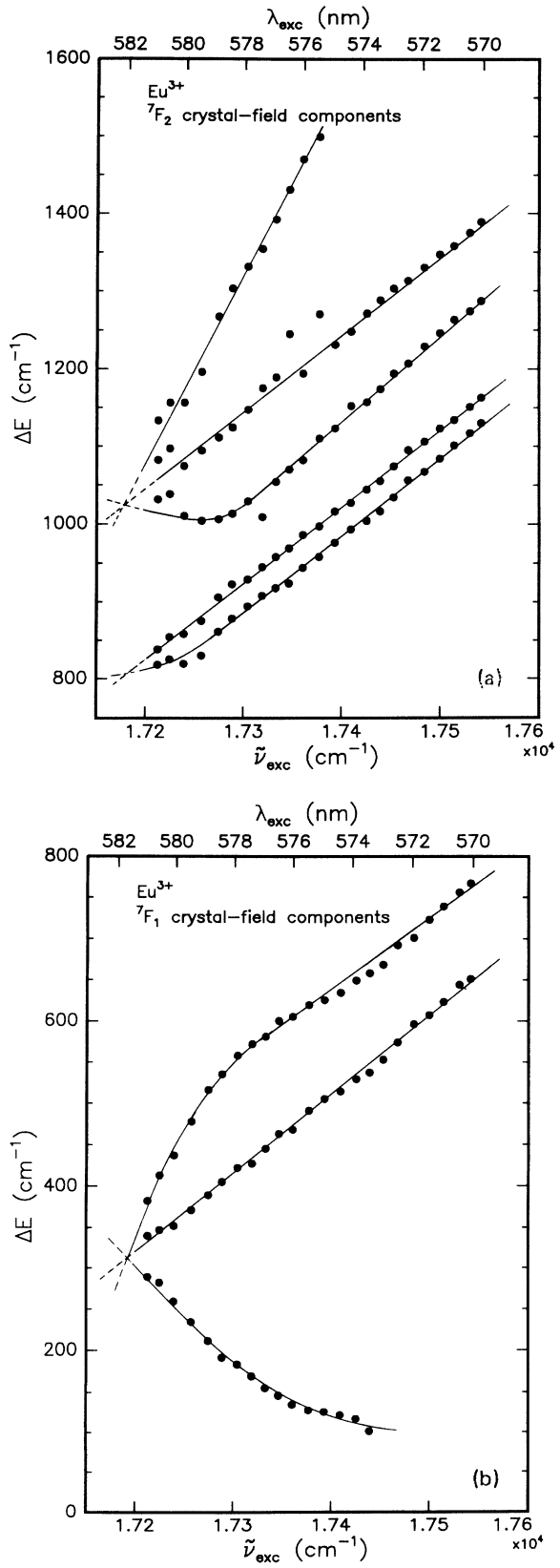

FIG. 4. Energy difference, ΔE, between the spectral positions of the individual components of the $^5D_0 \rightarrow {}^7F_1$ (a) and the $^5D_0 \rightarrow {}^7F_2$ (b) transitions of Eu^{3+} in silicate glass as a function of excitation energy, $\tilde{\nu}_{exc}$, within the $^5D_0 \leftarrow {}^7F_0$ absorption band, at 1.5 K.

THB-mechanism for both the Pr^{3+} and the Eu^{3+} samples is due to optical pumping of their nuclear hyperfine and quadrupole levels[9,23] which leads to short-lived holes (lifetimes of ms to min, depending on the temperature). The disappearance of these holes is caused by nuclear spin-lattice relaxation, as previously reported for crystals,[23,26] but the decay in glasses is much faster. This mechanism requires that the ground-state quadrupole splittings exceed the homogeneous linewidth, so that only sites for which this is true contribute to the holes.

We have studied transient holes in Pr^{3+} and Eu^{3+} in silicate glasses as a function of temperature and wavelength. From the shape and positions of very deep holes and antiholes we could get an estimate of the hyperfine and quadrupole splittings and their inhomogeneous distribution in the glass (Sec. III D). The lifetime of these transient holes decreases with increasing temperature.[21]

C. Holewidth as a function of excitation energy

The homogeneous linewidths, Γ_{hom}, as a function of excitation wavelength, λ_{exc}, within the inhomogeneously broadened absorption bands of the $^1D_2 \leftarrow {}^3H_4$ transition of Pr^{3+} and the $^5D_0 \leftarrow {}^7F_0$ transition of Eu^{3+}, at 1.2 K are plotted in Figs. 5(a) and 5(b).[21] For Pr^{3+}, $\Gamma_{hom} = (38 \pm 5)$ MHz, independent of λ_{exc} between 598 and 606 nm [Fig. 5(a)]. In addition, the decay of the $^1D_2$ fluorescence was found to be nonexponential, with a major lifetime component of 80 μs,[28] independent of λ_{exc}. These results are in contrast to those of Ref. 9, where an increase of Γ_{hom} from 250 to 850 MHz had been reported for the same wavelength region. The broadening in Ref. 9 was attributed to fast relaxation of the higher-lying crystal-field levels to the lowest one. We think that these discrepancies arise from the much higher burning-fluence densities used in Ref. 9. Since we could not burn holes at a wavelength below 597.5 nm, we believe that this is due to fast relaxation from higher excited crystal-field levels and that the holes in this region are too broad and shallow to be observed.

Eu^{3+}, on the contrary, does show an excitation-wavelength dependence of Γ_{hom} [Fig. 5(b)]. On the red wing of the absorption band, at 581 nm, $\Gamma_{hom} = (12 \pm 3)$ MHz, whereas on the blue wing, at 573 nm, $\Gamma_{hom} = (60 \pm 5)$ MHz, at 1.2 K. The slope $\Delta\Gamma_{hom}/\Delta\tilde{\nu}_{exc}$=0.19 MHz/cm^{-1} corresponds to a relative change with respect to Γ_{hom} of 1%/cm^{-1}. An increase of the homogeneous linewidth with decreasing λ_{exc} had previously been reported for Eu^{3+} in a variety of glasses at room temperature obtained by FLN.[2,5,16] Although the FLN experiments showed a much larger slope, $\Delta\Gamma_{hom}/\Delta\tilde{\nu}_{exc} \sim$ 1GHz/cm^{-1}, the relative change with respect to Γ_{hom} was also found to be $\sim$ 1%/cm^{-1}. The increase of Γ_{hom} with a decrease of λ_{exc} was interpreted in Ref. 16 in terms of a variation of the coupling strength between the rare-earth ion and the two-level systems of the glass with the lattice for different sites. This effect is further paralleled by a decrease of the fluorescence lifetime, τ, with decreasing λ_{exc}, as observed by Brecher and Riseberg.[17] The value of τ was defined in Ref. 17 as the major com-

ponent of a nonexponential decay of the $^5D_0$ level, which varied from 2.18 ms at 580 nm to 0.45 ms at 573 nm. These results were interpreted by associating an increase of the radiative transition probability with an apparent increase of the total crystal-field strength.[17] Thus, the varying crystal-field strength within the inhomogeneous linewidth seems to affect both the fluorescence lifetime of the $^5D_0$ state of Eu^{3+} and the homogeneous linewidth of the $^5D_0 \leftarrow {}^7F_0$ transition at room and at liquid-helium temperature. The linear dependence of Γ_{hom} on excitation energy extrapolates to $\Gamma_{hom} \sim 0$ at ~582 nm. This wavelength coincides with that obtained in Fig. 4 from the extrapolation of the splittings of the $^7F_1$ and $^7F_2$ components. At this spectral position the low-symmetry component of the crystal field is much smaller than that of the cubic component. The fact that $\Gamma_{hom} \sim 0$ implies that the Eu^{3+} ions sit in sites with no interacting TLS nearby.

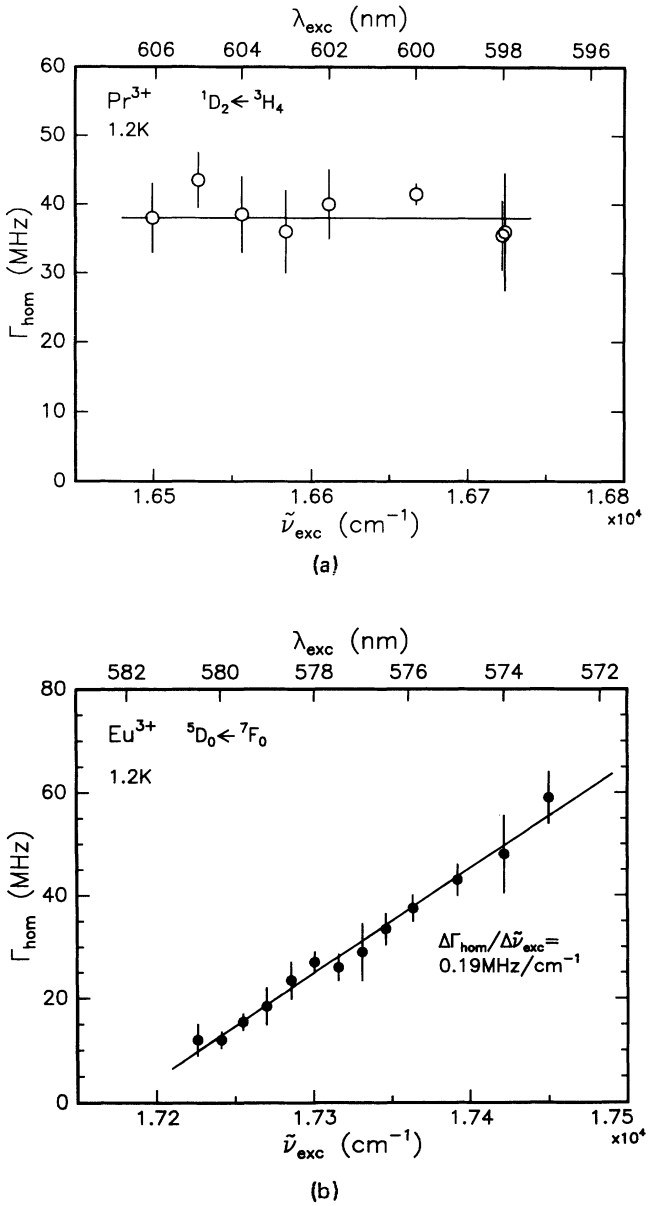

FIG. 5. Homogeneous linewidth, Γ_{hom}, as a function of excitation wavelength, λ_{exc}, within the $^1D_2 \leftarrow {}^3H_4$ transition of Pr^{3+} (a) and the $^5D_0 \leftarrow {}^7F_0$ transition of Eu^{3+} in silicate glasses (b), at 1.2 K.

D. Transient holes and antiholes: hyperfine structure

The shapes of three short-lived holes are shown in Fig. 6. The two upper profiles correspond to holes burnt into the $^5D_0 \leftarrow {}^7F_0$ transition of Eu^{3+} in silicate glass at 580 and 577 nm at 1.2 K, the bottom one to a hole burnt into the $^1D_2 \leftarrow {}^3H_4$ transition of Pr^{3+} at 606 nm at 0.4 K. On both sides of the deep resonant hole ($D \sim 20\%$) there appear symmetrically distributed antiholes, which are only observable if the holes have depths $D > 10\%$ [compare to Fig. 1(a)]. Such antiholes are characteristic of a hole-burning mechanism caused by optical pumping of nuclear hyperfine or quadrupole levels.[23] Whereas the hole resonant with the laser arises from depletion of a particular ground state, the symmetric antiholes are caused by enhanced population of the other ground-state hyperfine levels (see also Fig. 2, energy-level diagrams on the left). The frequency positions of the antiholes are given by the sums and differences of the hyperfine splittings in the ground and excited states.[22,23,26] Therefore, by comparison with hole-burning spectra of Eu^{3+} and Pr^{3+} in crystals,[23,26] we would expect a group of antiholes at a spectral distance within ~100 MHz from the resonant hole in Pr^{3+}, and two groups of antiholes within ~100 and ~300 MHz from the resonant hole in Eu^{3+} due to

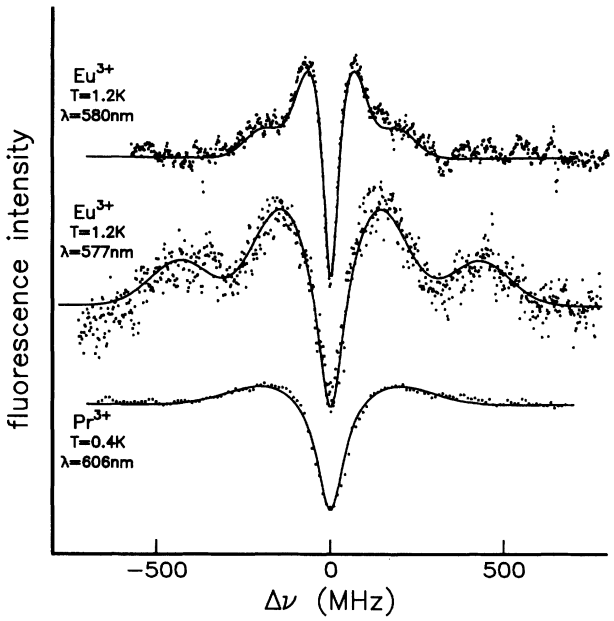

FIG. 6. Profile of deep resonant holes ($D \sim 20\%$) and antiholes burnt at 580 nm (top) and 577 nm (middle) in Eu^{3+}-doped silicate glass at 1.2 K, and at 606 nm (bottom) in Pr^{3+}-doped silicate glass at 0.4 K. The solid lines are fits to the data (see Sec. III D).

the two isotopes of europium, ^{151}Eu and ^{153}Eu, respectively. Since in a glass the homogeneous linewidth is much larger than in crystals and, in addition, the hyperfine splittings may vary from site to site giving rise to an inhomogeneous distribution, the antiholes are expected to be given by a superposition of nonresolved individual homogeneously broadened antiholes. The patterns shown in Fig. 6 have been interpreted by us in this way. In order to analyze the observed hole shapes, we have fitted the data with a Lorentzian hole resonant with the laser frequency and one or two pairs of Gaussian antiholes at a variable distance from this hole. Since the resonant holes are very deep ($D = 10-20\,\%$), their linewidths are power broadened by a factor of 2–4. We further observe that the widths of the antiholes are about 2–3 times larger than the Lorentzian resonant holes for both samples, at all temperatures and wavelengths measured. The positions of the antiholes for Eu^{3+} strongly depend on excitation wavelength (compare the two upper traces in Fig. 6). We also notice that the ratio between the frequency positions of the two antiholes in Eu^{3+} is about 1:3 at 1.2 K. If we compare the results for the two ions, we conclude (i) the values of the widths of holes and antiholes for Pr^{3+} are all a factor 4–5 larger than those for Eu^{3+} under similar conditions; (ii) there is only one antihole present on each side of the resonant hole in Pr^{3+}, whereas there are two in Eu^{3+}; (iii) there is no λ_{exc} dependence of the antihole position for Pr^{3+}, whereas there is for Eu^{3+}.

In Fig. 7 we have plotted the dependence of the antihole position with respect to the resonant hole as a function of excitation frequency, within the $^5D_0 \leftarrow {}^7F_0$ transition of Eu^{3+} at 1.2 K. Both antiholes display a linear shift of 0.77 MHz/cm^{-1} for one and of 2.4 MHz/cm^{-1} for the other.

The splitting of the $^7F_0$ state is due to the interaction between the nuclear quadrupole moment of Eu and the electric-field gradient of the environment. This splitting

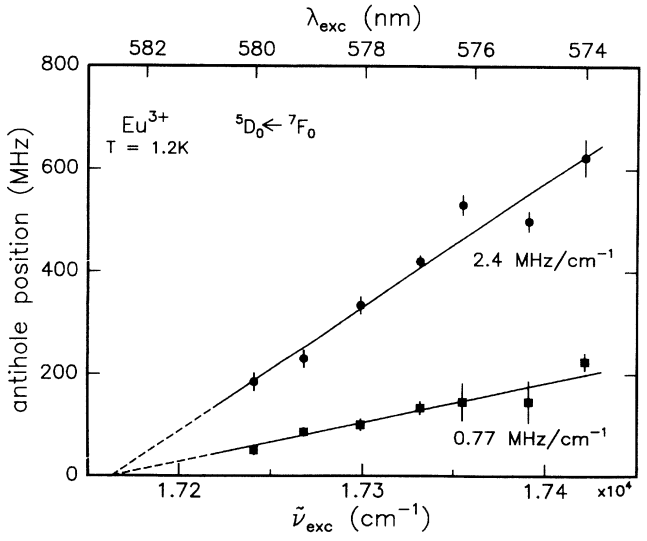

FIG. 7. Spectral positions of the two antiholes with respect to the resonant hole as a function of excitation energy, $\tilde{\nu}_{exc}$, for Eu^{3+} in silicate glass at 1.2 K. The two antiholes arise from the two europium isotopes, ^{151}Eu and ^{153}Eu.

is zero for a pure $J = 0$ state and requires an admixture of the $^7F_2$ state by the noncubic part of the crystal field, $H_{nc} = A_2^0(3z^2 - r^2)$.[29] The quadrupole splittings, E_Q, are then given by[29]

$$E_Q \propto \frac{\langle {}^7F_0|H_{nc}|{}^7F_2\rangle\langle {}^7F_2|H_Q|{}^7F_0\rangle}{E({}^7F_2 - {}^7F_0)} \quad , \tag{1}$$

where H_Q is the quadrupole-interaction term proportional to the quadrupole moment of each isotope of Eu, and the energy denominator ($\sim$1000 cm^{-1}) is the separation between the $J_z = 0$ component of the $^7F_2$ and $^7F_0$ levels. The excited $^5D_0$ state is less affected by such a perturbation because of the large energy difference between the $^5D_2$ and $^5D_0$ levels ($\sim$4300 cm^{-1}). There is also a pseudoquadrupole contribution to the splitting which is a second-order hyperfine interaction, but this is much smaller than the pure quadrupole term[29,30] and can be neglected. The observed variation of quadrupole splittings with excitation wavelength (Fig. 7) is not due to the wavelength dependence of the energy denominator in Eq. (1), which is approximately 1 part in 10^3 [Fig. 4(b)], but rather due to the variation of the strength of the noncubic crystal field, A_2^0. From the linear variation of the sidehole-splitting with excitation energy across the $^5D_0 \leftarrow {}^7F_0$ band we conclude that A_2^0 also varies linearly across this band. This is consistent with the close-to-linear variation of the splittings of the $^7F_1$ and $^7F_2$ states shown in Fig. 4, where these splittings are seen to collapse towards the long-wavelength edge of the absorption band and where the environment around the Eu^{3+} ions is evidently almost cubic. In this case one expects the quadrupole splittings and the $^7F_1$ splittings to vanish and the $^7F_2$ splitting to be determined by the cubic part of the crystal field which seems to be weak.

Since the two isotopes of Eu^{3+} have different quadrupole moments, Q, with a ratio $Q(^{153}\text{Eu})/Q(^{151}\text{Eu})$=2.556,[30] the expression for E_Q in Eq. (1) is different for each isotope. Thus, we would expect the position of the antihole corresponding to ^{153}Eu to shift about 2.5 times more than that of ^{151}Eu with respect to the excitation energy. In fact, we have measured a ratio of $\sim$3 between the slopes in Fig. 7, which agrees reasonably well with the assignment of the two groups of antiholes to the two isotopes ^{151}Eu and ^{153}Eu.

E. Optical dephasing

We have carried out a study of the homogeneous linewidth, Γ_{hom}, as a function of temperature for the $^1D_2 \leftarrow {}^3H_4$ transition of Pr^{3+} in a silicate glass between 0.4 and 12 K, and for the $^5D_0 \leftarrow {}^7F_0$ transition of Eu^{3+} in another silicate glass between 0.4 and 4.2 K. The results are shown in Fig. 8. As mentioned above, the value of Γ_{hom} for Pr^{3+} does not depend on the hole-burning mechanism. We could not detect holes for Eu^{3+} at $T > 4.2$ K because they decay in a time shorter than 50 ms, which was the time resolution of our experimental setup.

The best fit to the Pr^{3+} data is a power law with $\Gamma_{hom} = (30\pm2)\,T^{1.3\pm0.1}$ MHz over the whole temperature

range between 0.4 and 12 K. The discrepancy between these results and the linear temperature dependence of $\Gamma_{\rm hom}$ previously reported[9,19] can be understood if we take into account the dependence of $\Gamma_{\rm hole}$ on burning-fluence density [see Fig. 1(b)]. Recently a similar $T^{1.2\pm0.1}$ dependence was found for Pr^{3+} in yttria-stabilized-zirconia.[31] For Eu^{3+} in silicate glass, however, $\Gamma_{\rm hom}$ increases linearly with temperature,

$$\Gamma_{\rm hom} = (9 \pm 1)T^{(1.0\pm0.1)}\ \text{MHz},$$

between 0.4 and 4.2 K. We note that, as for Pr^{3+}, the values of $\Gamma_{\rm hom}$ reported earlier for Eu^{3+} (Refs. 9 and 19) were more than 30% larger than the present ones due to the larger burning-fluence densities used [see Fig. 1(b)].

In the inset of Fig. 8 a plot of $\Gamma_{\rm hom}$ versus temperature between 0.4 and 1.2 K is shown in more detail. $\Gamma_{\rm hom}$ extrapolates approximately to zero for both samples for $T \to 0$ K, within the laser jitter of 2 MHz. Other sources of dephasing such as population decay or nuclear spin flips[23] are much less than 1 MHz and cannot be observed with our resolution.

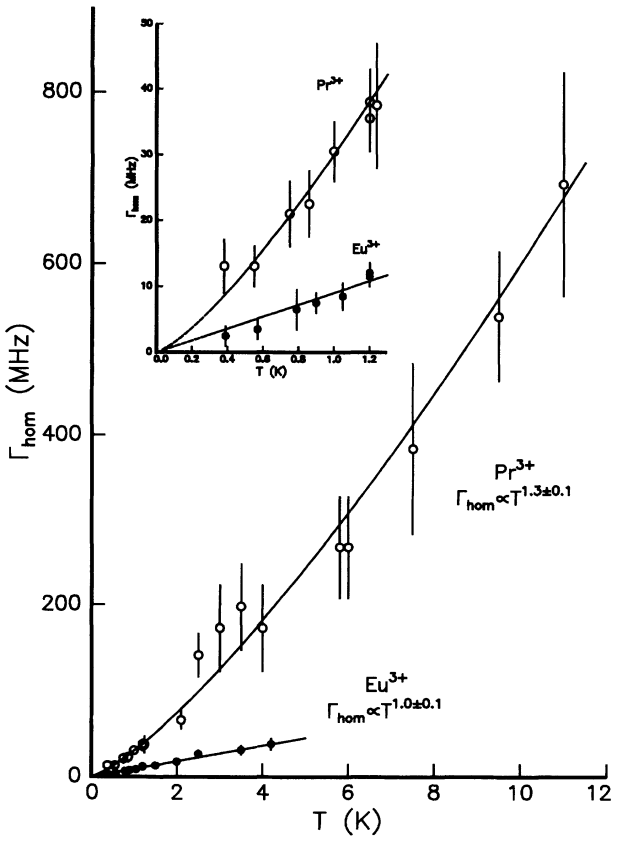

FIG. 8. Homogeneous linewidth, $\Gamma_{\rm hom}$, as a function of temperature for Pr^{3+}-doped between 0.4 and 12 K (open circles) and for Eu^{3+}-doped silicate glasses between 0.4 and 4.2 K (full circles). The burning wavelength was 606 nm for Pr^{3+} and 580 nm for Eu^{3+}. The solid lines represent fits to the data with $\Gamma_{\rm hom} = (30 \pm 2)T^{1.3\pm0.1}$ for Pr^{3+} and $\Gamma_{\rm hom} = (9 \pm 1)T^{1.0\pm0.1}$ for Eu^{3+}. Inset: $\Gamma_{\rm hom}$ vs T for both samples between 0.4 and 1.2 K. The data extrapolate to $\Gamma_{\rm hom} \sim 0$ for $T \to 0$ K, within the accuracy of the experiment (~2 MHz).

It is interesting that the optical homogeneous linewidth for Pr^{3+} shows a $T^{1.3\pm0.1}$ dependence between 0.4 and 12 K, whereas that for Eu^{3+} yields a linear T dependence between 0.4 and 4.2 K. The exact power law of the temperature dependence of $\Gamma_{\rm hom}$ is supposed to depend on the variation with energy of the density of states of the two-level systems of the glass.[14,15] The latter can be deduced from the temperature dependence of the specific heat.[32] It has been shown that if the density of states, ρ, varies with energy as $\rho dE \propto E^{\mu}dE$, the contribution of the TLS to the specific heat, $C_v^{\rm TLS}$, varies with temperature as $C_v^{\rm TLS} \propto T^{1+\mu}$.[32] The homogeneous linewidth should then vary as $\Gamma_{\rm hom} \propto T^{\alpha}$, where the relation between α and μ is given by:[14]

$$\alpha = (1+\mu)\frac{n}{3}. \tag{2}$$

In Eq. (2) n depends on the type of coupling between the optical center and the surrounding two-level systems. For an elastic (strain) dipole-dipole coupling ($n = 3$), which is generally assumed,[14,15] $\Gamma_{\rm hom}$ should show the same temperature dependence as $C_v^{\rm TLS}$.

In order to unravel the difference in the temperature dependence of $\Gamma_{\rm hom}$ for the two samples, specific heat experiments were carried out as a function of temperature on the same samples between 0.1 and 15 K.[33,34] The results of $C_v^{\rm TLS}$ are drawn in Figs. 9(a) and 9(b) in a double-logarithmic plot together with those of $\Gamma_{\rm hom}$.[33] For the Pr^{3+}-doped silicate glass we found $C_v^{\rm TLS} = (9.6 \pm 0.1)T^{1.29\pm0.02}\mu$ J/g K between 0.1 and 15 K, whereas for the Eu^{3+}-doped silicate glass,

$$C_v^{\rm TLS} = (3.5 \pm 0.1)T^{1.01\pm0.02}\mu\text{J/g K}$$

between 0.1 and 8 K.[33] The results agree with theoretical predictions[14] if we assume that the TLS density of states varies with energy according to $\rho dE \propto E^{\mu}dE$ with μ=0.3 for the Pr^{3+}-doped glass, and μ =0 for the Eu^{3+}-doped glass. We attribute the differences in the T dependences of $\Gamma_{\rm hom}$ for the two samples to differences in the composition of the two silicate glasses.[33]

F. Time dependence of the holewidth

Figure 10 shows values of the "effective" homogeneous linewidth, $\Gamma_{\rm hom}$ (see Sec. II), as a function of the logarithm of the experimental time scale, $t_{\rm expt}$. The latter, which is defined here as the sum of the burning time and the delay between burning and probing the hole, was varied between 70 ms and 100 s for the Pr^{3+}-doped and between 20 ms and 20 s for the Eu^{3+}-doped sample at 1.2 K. The lower limit of $t_{\rm expt}$ is given by the maximum scan speed of our HB apparatus, whereas the upper limit is determined by the hole-decay time of the transient holes. The results of Fig. 10 show no indication of hole broadening within the time span of three decades measured. This was confirmed for various temperatures between 0.4 and 1.2 K, and suggests that there is no spectral diffusion in these silicate glass samples between 10^{-2} and 10^{2} s.

No experimental time dependence of Γ_{hom} had previously been found either for the same Pr^{3+} sample by comparing hole-burning data at t_{expt}=100 s with accumulated photon-echo data at t_{expt} = 100 μs.[9] By contrast, low-temperature spectral diffusion processes seem to occur in a Nd^{3+}-doped silica glass fiber in a time scale of 100 ns as compared to 100 s. This was concluded from a two-pulse ns-photon-echo experiment (t_{expt}=100 ns) as compared to a 3-pulse-echo (Ref. 35) and spectral hole-burning experiments (t_{expt}=100 s).[36] Recently, spectral diffusion has also been observed for an Eu^{3+}-doped silicate glass fiber[37] by two-level hole-burning experiments on a microsecond time scale as compared to hole burning by optical pumping on a time scale of 1 s. Since the holes in Ref. 37 broadened by a factor of 2 over 6 orders of magnitude in time, it is possible that in the present samples we have not covered a large enough time span to be able to observe spectral diffusion.

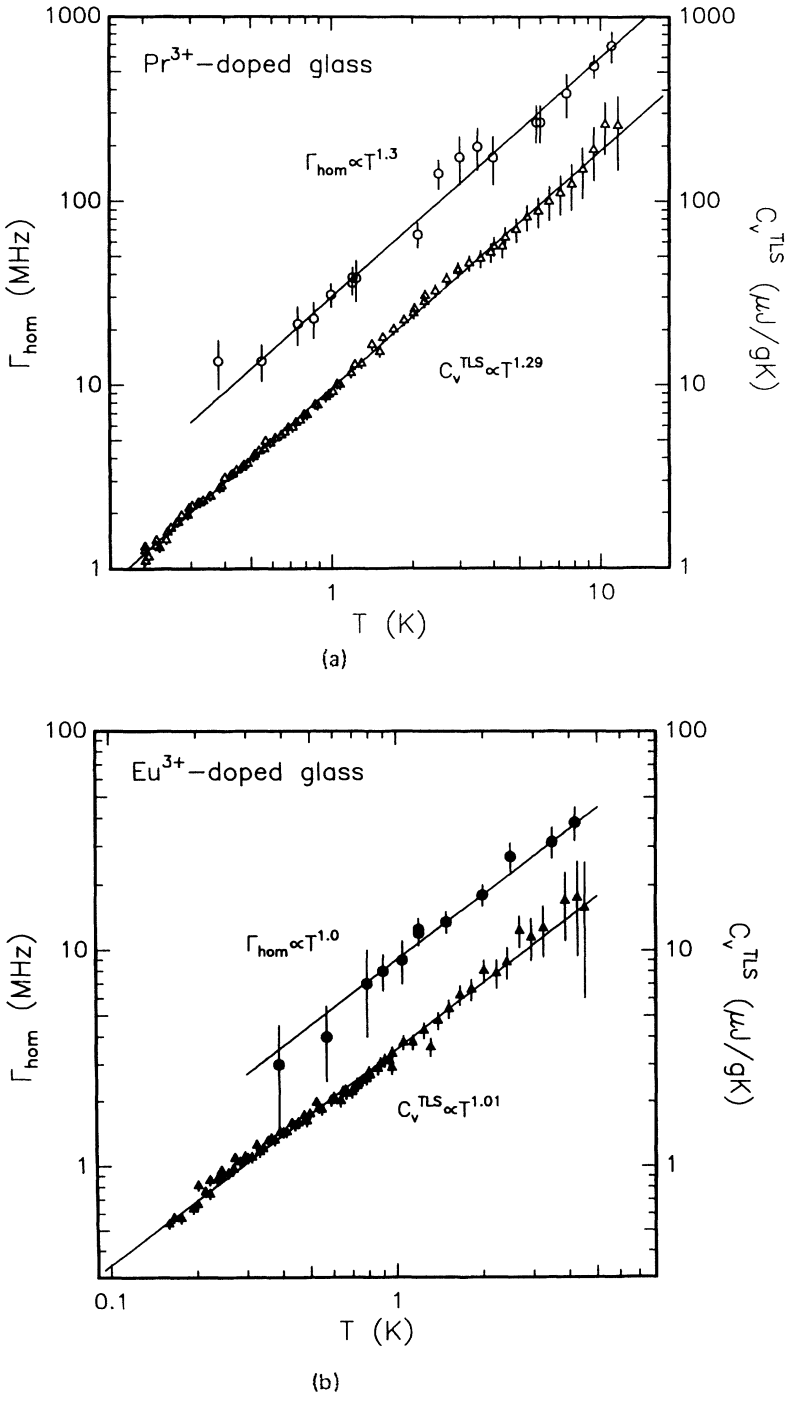

FIG. 9. (a) Homogeneous linewidth, Γ_{hom} (circles, left scale), and contribution of the two-level systems to the specific heat, C_v^{TLS} (triangles, right scale), as a function of temperature for Pr^{3+}-doped silicate glass, $\Gamma_{hom} = (30 \pm 2)T^{(1.3\pm0.1)}$ MHz between 0.4 and 12 K and $C_v^{TLS} = (9.6 \pm 0.1)T^{(1.29\pm0.02)}$ μJ/g K between 0.1 and 15 K. (b) As (a) for Eu^{3+}-doped silicate glass, $\Gamma_{hom} = (9 \pm 1)T^{(1.0\pm0.1)}$ MHz between 0.4 and 4.2 K, and $C_v^{TLS} = (3.5 \pm 0.1)$ $T^{(1.01\pm0.02)}$ μJ/g K between 0.1 and 8 K (see Ref. 33).

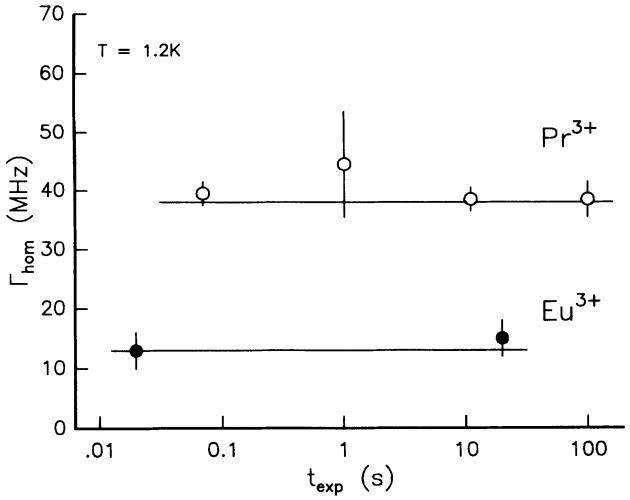

FIG. 10. Homogeneous linewidth, Γ_{hom}, as function of experimental time scale, t_{expt}, for Pr^{3+} (open circles) and Eu^{3+} (full circles) in silicate glasses at 1.2 K between 10^{-2} and 10^{2} s.

IV. CONCLUSIONS

Our results show that the optical dynamic behaviour of Pr^{3+} in a silicate glass is quite different from that of Eu^{3+} in another silicate glass at low temperature. We have observed no dependence of Γ_{hom} on excitation energy for Pr^{3+}, while we did observe such a dependence for Eu^{3+} with a broadening of $\Delta\Gamma_{hom}/\Delta\tilde{\nu}_{exc}=0.19$ MHz/cm^{-1}. Since the relative increase of Γ_{hom} with excitation energy within the inhomogeneous linewidth is about 1%/cm^{-1} at liquid-helium as well as at room temperature, the results suggest that the broadening in both cases is due to the same mechanism. We propose for it the variation of the strength of the noncubic component of the crystal field within the $^5D_0 \leftarrow {}^7F_0$ transition of Eu^{3+}.

We found that two types of hole-burning processes are active for Pr^{3+} in silicate glass, a persistent and a transient one, whereas only transient hole burning has been observed for Eu^{3+} in silicate glass. The mechanism responsible for transient hole burning is optical pumping of nuclear hyperfine and quadrupole levels, while that for persistent hole burning is probably a slight rearrangement of the local structure of the glass in the vicinity of the rare-earth ion. We have fitted the hole shapes of deeply burnt transient holes with a simple model from which we have obtained the distribution of the hyperfine levels in the glass. Further, from the shift of the antiholes with excitation energy observed for Eu^{3+} we concluded that the strength of the noncubic component of the crystal field varies linearly with excitation energy. We have also identified the contribution to the hole-antihole pattern as due to the two isotopes of Eu, ^{151}Eu, and ^{153}Eu, because of their different quadrupole moments. This is the first time, to our knowledge, that the spectroscopic structure due to the two isotopes has been distinguished in a glass.

The "effective" homogeneous linewidth, Γ_{hom}, follows a $T^{(1.3\pm0.1)}$ dependence for Pr^{3+} in a silicate glass, whereas $\Gamma_{hom} \propto T^{(1.0\pm0.1)}$ for Eu^{3+} in a silicate glass of different composition. For comparison, the contribution to the specific heat of the two-level systems, C_v^{TLS}, follows a $T^{(1.29\pm0.02)}$ dependence for the Pr^{3+}-doped sample and a $T^{(1.01\pm0.02)}$ dependence for the Eu^{3+}-doped sample in the same temperature region. These results corroborate theoretical models of optical dephasing in which the same T dependence is predicted for both Γ_{hom} and C_v^{TLS} in a given sample.

Finally, we have observed no influence of the time scale of the experiment on the holewidth between 10^{-2} and 10^{2} s for the two rare-earth-doped silicate glasses. Thus, spectral diffusion does not seem to play a role in these samples within this time-span.

ACKNOWLEDGMENTS

We thank P. J. van der Zaag and B. C. Schokker for their efforts in the early phases of this study.[21] We further acknowledge R. Wannemacher for useful discussions on the physics of rare-earth ions. The investigations were supported by the Netherlands Foundation for Physical Research (FOM) and Chemical Research (SON) with financial aid from the Netherlands Organization for Scientific Research (NWO).

* Present address: Institute for Biophysics, University of Linz, 4040 Linz, Austria.
† Author to whom correspondence should be addressed.

[1] P.M. Selzer, D.L. Huber, D.S. Hamilton, W.M. Yen, and M.J. Weber, Phys. Rev. Lett. **36**, 813 (1976).
[2] P. Avouris, A. Campion, and M.A. El-Sayed, J. Chem. Phys. **67**, 3397 (1977).
[3] J. Hegarty and W.M. Yen, Phys. Rev. Lett. **43**, 1126 (1979).
[4] J.M. Pellegrino, W.M. Yen, and M.J. Weber, J. Appl. Phys. **51**, 6332 (1980).
[5] J.R. Morgan and M.A. El-Sayed, Chem. Phys. Lett. **84**, 213 (1981).
[6] G.S. Dixon, R.C. Powell, and X. Gang, Phys. Rev. B **33**, 2713 (1986).
[7] R.T. Brundage and W.M. Yen, Phys. Rev. B **33**, 4436 (1986).
[8] R.M. Shelby, Opt. Lett. **8**, 46 (1983).
[9] R.M. Macfarlane and R.M. Shelby, Opt. Commun. **45**, 46 (1983).
[10] J. Hegarty, M.M. Broer, B. Golding, F.R. Simpson, and F.B. MacChesney, Phys. Rev. Lett. **51**, 2033 (1983).
[11] S. Völker, in *Relaxation Processes in Molecular Excited States,* edited by J. Fünfschilling (Kluwer, Dordrecht, 1989), p. 113, and references therein; Annu. Rev. Phys. Chem. **40**, 499 (1989), and references therein.

[12] H. van der Laan and S. Völker (unpublished); H. van der Laan, Ph.D. thesis, University of Leiden, 1992, Chap. 4.
[13] R. van der Berg and S. Völker, Chem. Phys. Lett. **150**, 491 (1988).
[14] D.L. Huber, M.M. Broer, and B. Golding, Phys. Rev. Lett. **52**, 2281 (1984).
[15] For reviews on theoretical models of dephasing in glasses, see *Optical Linewidths in Glasses*, edited by M.J. Weber, J. Lumin. **36**, 179 (1987); R. Silbey, in *Relaxation Processes in Molecular Excited States,* edited by J. Fünfschilling (Kluwer, Dordrecht, 1989), p. 235, and references therein.
[16] J.R. Morgan, E.P. Chock, W.D. Hopewell, M.A. El-Sayed, and R. Orbach, J. Chem. Phys. **85**, 80 (1981).
[17] C. Brecher and L.A. Riseberg, Phys. Rev. B **13**, 81 (1976).
[18] P.J. van der Zaag, J.P. Galaup, and S. Völker, Chem. Phys. Lett. **166**, 263 (1990).
[19] P.J. van der Zaag, B.C. Schokker, Th. Schmidt, and S. Völker, L. Lumin. **45**, 80 (1990).
[20] H.P.H. Thijssen, R. van den Berg, and S. Völker, Chem. Phys. Lett. **120**, 503 (1985).
[21] P.J. van der Zaag, Ph.D. thesis, University of Leiden, 1992, Chap. 6.
[22] R.M. Shelby, R.M. Macfarlane, and C.S. Yannoni, Phys. Rev. B **21**, 5004 (1980).
[23] R.M. Macfarlane and R.M. Shelby, in *Spectroscopy of Solids Containing Rare-Earth Ions*, edited by A.A. Kaplyanskii and R.M. Macfarlane (North-Holland, Amsterdam, 1987), p. 51, and references therein.
[24] W.R. Babbit, A. Lezama, and T.W. Mossberg, Phys. Rev. B **39**, 1987 (1989).
[25] R.M. Shelby and R.M. Macfarlane, Phys. Rev. Lett. **47**, 1172 (1981).
[26] R.M. Macfarlane, R.M. Shelby, A.Z. Genack, and D.A. Weitz, Opt. Lett. **5**, 462 (1980); R.M. Macfarlane and R.M. Shelby, *ibid.* **6**, 96 (1980).
[27] C. Brecher and L.A. Riseberg, Phys. Rev. B **21**, 2607 (1980).
[28] C. De Caro and R. Wannemacher (private communication).
[29] R.J. Elliot, Proc. Phys. Soc. London, Ser. B **70**, 119 (1957).
[30] A.J. Silversmith and N.B. Manson, Phys. Rev. B **34**, 4854 (1986).
[31] K. Tanaka, T. Okuno, H. Yugami, M. Ishigame, and T. Suemoto, Opt. Commun. **86**, 45 (1991).
[32] J.C. Lasjaunis, A. Ravex, M. Vandorpe, and S. Hunklinger, Solid State Commun. **17**, 1095 (1975).
[33] Th. Schmidt, J. Baak, B. van der Straat, H. Brom, and S. Völker, Phys. Rev. Lett. **71**, 3031 (1993).
[34] The specific heat experiments have been performed in the group of H. Brom, Kamerlingh Onnes Laboratory, University of Leiden.
[35] M.M. Broer, B. Golding, W.H. Haemmerle, J.R. Simpson, and D.L. Huber, Phys. Rev. B **33**, 4160 (1986).
[36] W.S. Brocklesby, B. Golding, and J.R. Simpson, Phys. Rev. Lett. **63**, 1833 (1989).
[37] R. Wannemacher, J.M.A. Koedijk, and S. Völker, J. Lumin. **60**, 437 (1994).